Explanation-Consistency Graphs: Neighborhood Surprise in Explanation Space for Training Data Debugging

Anonymous ACL submission

Abstract

Training data quality is critical for NLP model performance, yet identifying mislabeled examples remains challenging when models confidently fit errors via spurious correlations. Confident learning methods like Cleanlab assume mislabeled examples cause low confidence; however, this assumption breaks down when artifacts enable confident fitting of wrong labels. We propose **Explanation-Consistency Graphs (ECG)**, which detects problematic training instances by computing neighborhood surprise in *explanation embedding space*. Our key insight is that LLM-generated explanations capture "why this label applies," and this semantic content reveals inconsistencies invisible to classifier confidence. By embedding structured explanations and measuring k-nearest neighbor (kNN) label disagreement, ECG achieves 0.832 area under the ROC curve (AUROC) on artifact-aligned noise (where Cleanlab drops to 0.107), representing a 24% improvement over the same algorithm on input embeddings (0.671). On random label noise, ECG remains competitive (0.943 vs. Cleanlab's 0.977), demonstrating robustness across noise regimes. We show that the primary value lies in the *explanation representation* rather than complex signal aggregation, and analyze why naive multi-signal combination can degrade performance when training dynamics signals are anti-correlated with artifact-driven noise.

1 Introduction

The quality of training data fundamentally constrains what NLP models can learn. Large-scale empirical studies reveal label error rates ranging from 0.15% (MNIST) to 5.83% (ImageNet), averaging 3.3% across 10 benchmark test sets (Northcutt et al., 2021b), and these errors propagate into systematic model failures. Beyond simple mislabeling, annotation artifacts and spurious correlations create particularly insidious data quality issues: models learn superficial patterns that happen to correlate with labels in the training set but fail catastrophically under distribution shift (Gururangan et al., 2018; McCoy et al., 2019). Identifying and correcting such problematic instances, known as *training data debugging*, is therefore essential for building reliable NLP systems.

The dominant paradigm for training data debugging relies on model confidence and loss signals. **Confident learning** (Northcutt et al., 2021a) estimates a joint distribution between noisy and true labels using predicted probabilities, effectively identifying instances where the model "disagrees" with the observed label. **Training dynamics** approaches like AUM (Pleiss et al., 2020) and CTRL (Yue and Jha, 2022) track per-example margins and loss trajectories across training epochs, exploiting the observation that mislabeled examples exhibit different learning patterns than clean ones. High-loss filtering with pretrained language models can be surprisingly effective on human-originated noise (Chong et al., 2022). These methods share a common assumption: *problematic examples will cause low confidence or high loss during training*.

This assumption breaks down catastrophically when **models confidently fit errors via spurious correlations**. Consider sentiment data where mislabeled examples happen to contain distinctive tokens such as rating indicators like "[RATING=5]", demographic markers, or formatting artifacts. The classifier learns to predict the *wrong* labels with *high confidence* by exploiting these spurious markers. From a loss perspective, these mislabeled examples look perfectly clean; they are fitted early, with high confidence, and low loss throughout training. Cleanlab's confident joint and AUM's margin trajectories both fail because the model is confident, just confidently wrong for the wrong reasons.

This failure mode is not hypothetical. Poliak et al. (2018) showed that NLI datasets can be partially solved using only the hypothesis, revealing pervasive annotation artifacts. Gururangan et al.

(2018) demonstrated that annotation patterns systematically correlate with labels in ways that models exploit. The spurious correlation literature extensively documents how models learn shortcuts that evade standard diagnostics (Clark et al., 2019; Utama et al., 2020; Tu et al., 2020), and debiasing methods must explicitly model bias structure to mitigate it (Sagawa et al., 2020). When the very mechanism that causes label noise *also* enables confident fitting, confidence-based debugging becomes unreliable.

We propose **Explanation-Consistency Graphs (ECG)**, which detects problematic training instances by computing neighborhood surprise in *explanation embedding space* rather than input embedding space. Our key insight is that *explanations encode semantic information about why a label should apply*, and this "why" content reveals inconsistencies even when classifier confidence does not. When an LLM explains why it believes a sentence has positive sentiment, its rationale and cited evidence reflect the actual semantic content, not spurious markers that the classifier may have learned to exploit. By embedding these explanations and measuring kNN label disagreement, ECG detects mislabeled instances that are invisible to loss and probability signals.

The core idea is simple: if an example's label disagrees with the labels of examples whose *explanations* are most similar, that label is likely wrong. This is the same principle underlying input-based kNN detection (Bahri et al., 2020; Kim et al., 2023), but operating in a fundamentally different representation space. Input embeddings capture "what the text is about"; explanation embeddings capture "why this text has this label." When labels are wrong, the "why" becomes inconsistent with semantically similar examples, making explanation-space neighborhood surprise a powerful detection signal.

ECG synthesizes ideas from three research threads: **(1)** the explanation-based debugging literature, which uses explanations to help humans surface artifacts (Lertvittayakumjorn and Toni, 2021; Lertvittayakumjorn et al., 2020; Lee et al., 2023), but has not automated detection via graph structure; **(2)** graph-based noisy label detection, which uses neighborhood disagreement in representation space (Bahri et al., 2020; Kim et al., 2023; Di Salvo et al., 2025), but over input embeddings; and **(3)** LLM-generated explanations with structured schemas (Geng et al., 2023; Huang et al., 2023), which provide the semantic substrate for our graph.

Concretely, ECG works as follows. **(1) Explanation Generation:** We generate structured JSON explanations for all training instances using an instruction-tuned LLM (Qwen3-8B), enforcing JSON structure via schema-constrained decoding and instructing the model to quote extractive evidence spans. **(2) Explanation Embedding:** We embed explanations using a sentence encoder and construct a kNN graph in this space. **(3) Neighborhood Surprise:** We compute the negative log-probability of each instance's label given its neighbors' labels in explanation space, which serves as our primary detection signal. We also explored additional signals (NLI contradiction, stability, training dynamics), but found that simple kNN surprise in explanation space works best.

Our contributions are:

1. We introduce **Explanation-Consistency Graphs (ECG)**, demonstrating that neighborhood surprise computed in *explanation embedding space* substantially outperforms the same algorithm on input embeddings (+24% AUROC on artifact-aligned noise, i.e., mislabeling paired with spurious markers that enable confident fitting: 0.832 vs. 0.671).

2. We establish a **concrete failure mode** for confidence-based cleaning: when artifacts enable confident fitting of wrong labels, Cleanlab achieves only 0.107 AUROC (worse than random), while ECG achieves 0.832. ECG remains competitive on random noise (0.943 vs. Cleanlab's 0.977), providing a **robust** method across noise regimes.

3. We provide **analysis of why naive signal aggregation fails**: training dynamics signals (AUM) are anti-correlated with noise under artifact conditions, because artifacts make wrong labels *easy* to learn. This negative result offers guidance for future multi-signal approaches.

2 Related Work

ECG targets training-data debugging in a regime where spurious correlations let models fit wrong labels *confidently*. It connects to (i) label-error detection from confidence and training dynamics, (ii) graph-based data quality, and (iii) explanation-

and attribution-based diagnosis of artifacts. Across these areas, the key gap is a scalable detector whose signal remains informative when classifier confidence is *not*.

2.1 Label-Error Detection Under Confident Fitting

Most data-cleaning methods rank examples using signals derived from the classifier. **Confident learning** (Northcutt et al., 2021a) identifies likely label errors via disagreement between observed labels and predicted probabilities, and works well when noise manifests as low confidence. Training-dynamics methods similarly treat mislabeled data as hard-to-learn: **AUM** (Pleiss et al., 2020) uses cumulative margins, and **CTRL** (Yue and Jha, 2022) clusters loss trajectories to separate clean from noisy examples. For NLP, out-of-sample loss ranking with pretrained language models can be highly effective on human-originated noise (Chong et al., 2022).

Gap. These approaches share a reliance on training-time difficulty (high loss, low margin, or low confidence). When artifacts make wrong labels easy to fit, mislabeled instances can have *low loss and high confidence* throughout training, rendering confidence- and dynamics-based detectors unreliable. ECG addresses this failure mode by using a signal derived from *explanations* rather than the classifier's fit.

2.2 Graph-Based Data Quality and Neighborhood Disagreement

Graph-based methods detect label errors from representation-space structure, flagging instances whose labels disagree with their nearest neighbors. This principle appears in kNN-based noisy-label detection (Bahri et al., 2020) and scalable relation-graph formulations that jointly model label errors and outliers (Kim et al., 2023). Recent work improves robustness when errors cluster, e.g., reliability-weighted neighbor voting (Di Salvo et al., 2025), and label propagation on kNN graphs when clean anchors exist (Iscen et al., 2020).

Gap. Prior graph-based approaches build neighborhoods over input embeddings or model representations. ECG keeps the same neighborhood-disagreement idea but changes the substrate: it constructs the graph in *explanation embedding space*, where neighbors are defined by similar *label-justifying evidence and rationales*. This shift is crucial in artifact-aligned settings, where input-space similarity can preserve spurious markers rather than the underlying "why" of the label.

2.3 Explanations, Artifacts, and Dataset Debugging

Explanations and attribution have been used extensively for diagnosing dataset artifacts and guiding model fixes. Surveyed "explanation → feedback → fix" pipelines (Lertvittayakumjorn and Toni, 2021) and interactive systems such as **FIND** (Lertvittayakumjorn et al., 2020), explanation-driven label cleaning (Teso et al., 2021), and **XMD** (Lee et al., 2023) support human-in-the-loop debugging. Complementarily, training-set artifact analyses localize influential tokens and examples, e.g., **TFA** (Pezeshkpour et al., 2022) and influence-function based artifact discovery (Han et al., 2020). These tools are motivated by a broad literature on spurious correlations and annotation artifacts, including hypothesis-only shortcuts in NLI and debiasing or counterfactual remedies (Poliak et al., 2018; Belinkov et al., 2019; Clark et al., 2019; Utama et al., 2020; Kaushik et al., 2020).

Gap. Existing explanation-based debugging largely supports *human* discovery or *model* regularization, while spurious-correlation work typically targets mitigation rather than identifying which *training instances* are mislabeled. To our knowledge, ECG is the first to aggregate LLM explanations via graph structure for automated data cleaning, bridging the explanation and data-quality literatures.

LLM-generated explanations. Because ECG relies on structured LLM explanations as a representation, we summarize related work on structured generation and explanation reliability in Appendix C.

3 Method

Given a training dataset $\mathcal{D} = \{(x_i, y_i)\}_{i=1}^{n}$ with potentially noisy labels y_i, our goal is to produce a suspiciousness ranking that places mislabeled or artifact-laden instances at the top. ECG achieves this through three stages: explanation generation (§3.1), explanation embedding and graph construction (§3.2), and neighborhood surprise computation (§3.3). Figure 1 provides an overview. We also explored additional signals (NLI contradiction, stability, training dynamics) but found they did not improve over simple neighborhood surprise; we analyze this in §6 and provide details in Appendix A.

3.1 Structured Explanation Generation

For each training instance x_i, we generate a structured JSON explanation using an instruction-tuned LLM (Qwen3-8B). The explanation contains:

- `pred_label`: The LLM's predicted label
- `evidence`: 1–3 exact substrings from x_i justifying the prediction
- `rationale`: A brief explanation ($\leq$25 tokens) without label words
- `counterfactual`: A minimal change that would flip the label
- `confidence`: Integer 0–100

We enforce schema validity via constrained decoding and instruct the LLM to ignore metadata tokens (e.g., `<lbl_pos>`) so explanations reflect semantic content rather than spurious markers.

Stability Sampling. LLM explanations can be unstable across random seeds. We generate $M = 3$ explanations per instance (one deterministic at temperature 0, two samples at temperature 0.7) and compute a **reliability score**:

$$\rho_i = \frac{1}{3}(L_i + E_i + R_i) \tag{1}$$

where L_i (label agreement), E_i (evidence Jaccard), and R_i (rationale similarity) each measure agreement across the M samples. High ρ_i indicates stable, reliable explanations; low ρ_i indicates the LLM is uncertain or the instance is ambiguous.

3.2 Reliability-Weighted Graph Construction

We embed explanations and construct a kNN graph that downweights unreliable neighbors, inspired by WANN (Di Salvo et al., 2025).

Explanation Embedding. For each instance, we form a canonical string t_i excluding label information:

$$t_i = \texttt{"Evidence: "} \oplus e_i \oplus \texttt{" | Rationale: "} \oplus r_i \tag{2}$$

where e_i and r_i are the evidence and rationale fields. We embed t_i using a sentence encoder (all-MiniLM-L6-v2) and L_2-normalize to obtain v_i.

Reliability-Weighted Edges. We retrieve the $k = 15$ nearest neighbors $\mathcal{N}(i)$ for each node using FAISS. Edge weights incorporate both similarity and neighbor reliability:

$$\tilde{w}_{ij} = \exp\left(\frac{s_{ij}}{\tau}\right) \cdot \rho_j, \quad w_{ij} = \frac{\tilde{w}_{ij}}{\sum_{j' \in \mathcal{N}(i)} \tilde{w}_{ij'}} \tag{3}$$

where $s_{ij} = v_i^\top v_j$ is cosine similarity, $\tau = 0.07$ is a temperature, and ρ_j is neighbor reliability. This ensures that unstable or unreliable neighbors contribute less to inconsistency signals.

Outlier Detection. We compute an outlier score $O_i = 1 - \frac{1}{k} \sum_{j \in \mathcal{N}(i)} s_{ij}$ to distinguish genuinely out-of-distribution examples from mislabeled in-distribution examples.

3.3 Neighborhood Surprise Detection

The core detection signal in ECG is **neighborhood surprise**: if an instance's label disagrees with the labels of instances with similar explanations, the label may be wrong.

Neighborhood Surprise (S_{nbr}). We compute a weighted neighbor label posterior with Laplace smoothing:

$$p_i(c) = \frac{\epsilon + \sum_{j \in \mathcal{N}(i)} w_{ij} \cdot \mathbf{1}[y_j = c]}{C\epsilon + 1} \tag{4}$$

where C is the number of classes and $\epsilon = 10^{-3}$. The suspiciousness score is then:

$$S_{\text{nbr}}(i) = -\log p_i(y_i) \tag{5}$$

High S_{nbr} indicates the observed label is unlikely given similar explanations. Instances are ranked by S_{nbr} and the top-K are flagged for removal or review.

Why Explanation Space? The same neighborhood surprise algorithm can be applied to input embeddings (ECG (input)) or explanation embeddings (ECG). The key empirical finding is that explanation embeddings yield substantially better detection:

- **ECG**: 0.832 AUROC on artifact-aligned noise
- **ECG (input)**: 0.671 AUROC (same algorithm, different embedding)

This 24% improvement demonstrates that explanations capture label-quality information invisible in input space. When labels are wrong, the LLM's

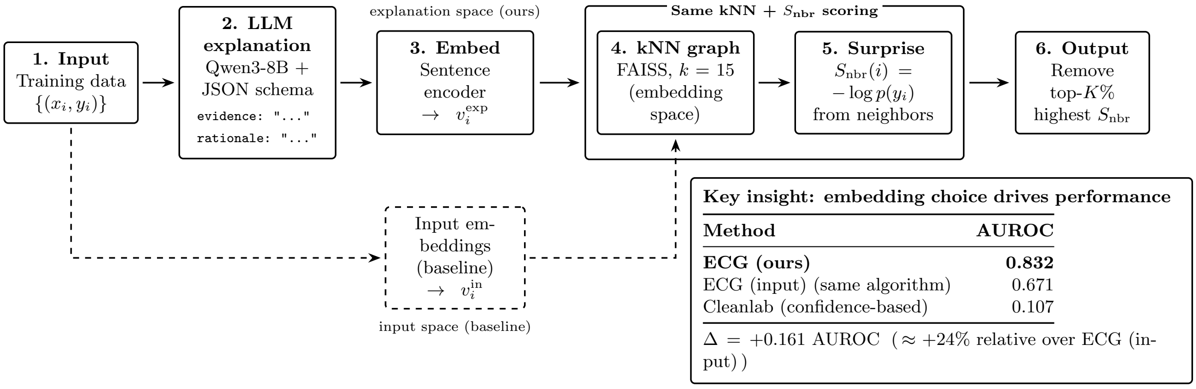

Key insight: embedding choice drives performance

Method	AUROC
ECG (ours)	**0.832**
ECG (input) (same algorithm)	0.671
Cleanlab (confidence-based)	0.107

Δ = +0.161 AUROC ($\approx$ +24% relative over ECG (input))

Figure 1: **ECG Pipeline.** Given training data with potentially noisy labels, ECG: (1) generates structured LLM explanations; (2) embeds the explanation text; (3) constructs a kNN graph in explanation space; (4) computes neighborhood surprise—the negative log-probability of each label given its neighbors. The key insight: the same kNN algorithm achieves **0.832 AUROC** on explanation embeddings vs. 0.671 on input embeddings (+24%), while Cleanlab fails completely (0.107) on artifact-aligned noise.

rationale reflects semantic inconsistency with similar examples, even if the input text is similar to correctly-labeled examples.

Explored Extensions. We also investigated additional signals: NLI contradiction (does the explanation contradict the label?), explanation stability (does the LLM give consistent explanations across samples?), and training dynamics (does the classifier struggle to learn this example?). Surprisingly, combining these signals with neighborhood surprise *degraded* performance on artifact-aligned noise. We analyze why in §6: the training dynamics signal is anti-correlated with noise when artifacts make wrong labels easy to learn. Details of all signals are in Appendix A.

4 Experimental Setup

4.1 Dataset and Noise Injection

We evaluate on **SST-2** (binary sentiment), subsampling 25,000 training examples. We create two synthetic noise conditions at rate $p = 10\%$:

Uniform Noise. Labels are flipped uniformly at random. This is a sanity check where confidence-based methods should excel.

Artifact-Aligned Noise. Labels are flipped *and* a spurious marker is appended: `<lbl_pos>` for (flipped) positive labels, `<lbl_neg>` for negative. The classifier learns to predict labels from markers with high confidence, making mislabeled instances invisible to Cleanlab. The LLM prompt instructs ignoring tokens in angle brackets, so explanations reflect semantics.

4.2 Baselines

We compare against:

- **Cleanlab**: Confident learning with 5-fold cross-validated probabilities (Northcutt et al., 2021a)
- **High-Loss**: Ranking by cross-entropy loss
- **AUM**: Area Under Margin from training dynamics (Pleiss et al., 2020)
- **LLM Mismatch**: Binary indicator of LLM $\neq$ observed label
- **ECG (input)**: Neighborhood surprise on input embeddings (same algorithm as ECG, different embedding space)
- **Random**: Random selection

4.3 Metrics

Detection. AUROC, AUPRC, Precision@K, Recall@K, F1@K for identifying noisy instances.

Downstream. Accuracy on clean test set; accuracy when artifacts are stripped or swapped at test time (out-of-distribution, OOD, robustness).

4.4 Implementation

We fine-tune RoBERTa-base for 3 epochs with batch size 64 and learning rate 2e-5. Explanations use Qwen3-8B (Team, 2025) via vLLM (Kwon et al., 2023) with constrained JSON decoding. NLI uses an ensemble of RoBERTa-large-MNLI and BART-large-MNLI. Experiments run on a single H100 GPU.

Method	AUROC	AUPRC	P@10%
Random	0.500	0.100	0.100
Confidence-Based Methods			
Cleanlab	0.107	0.056	0.000
High-Loss	0.107	0.056	0.000
AUM (Margin)	0.107	0.056	0.000
Embedding-Based Methods			
ECG (input)	0.671	0.258	0.342
LLM Mismatch	0.575	0.152	0.280
ECG Variants			
ECG (multi-signal)	0.547	0.117	0.154
ECG	**0.832**	**0.435**	**0.496**

Table 1: Detection performance on artifact-aligned noise (10% noise rate, N=25,000). Confidence-based methods (Cleanlab, Loss, AUM) drop below random (0.5 AUROC) because artifacts make mislabeled examples easy to fit. ECG achieves 0.832 AUROC—a 24% improvement over ECG (input) (0.671) using the same algorithm.

Method	AUROC	AUPRC
Cleanlab	**0.977**	**0.854**
LLM Mismatch	0.901	0.632
ECG (input)	0.880	0.492
ECG	0.943	0.724

Table 2: Detection on random noise (10%). Cleanlab excels as expected. ECG remains competitive (0.943), only 3.4% behind Cleanlab.

Method	Artifact	Random	Robust?
Cleanlab	0.107	**0.977**	✗
ECG (input)	0.671	0.880	✓
ECG	**0.832**	0.943	✓

Table 3: Robustness across noise regimes. Cleanlab fails on artifact noise (0.107) despite excelling on random noise (0.977). ECG is robust: best on artifacts, competitive on random.

5 Results

5.1 Detection Performance on Artifact-Aligned Noise

Table 1 shows detection metrics on artifact-aligned noise, where mislabeled examples contain spurious markers that enable confident classifier fitting. This is the failure mode for confidence-based methods: the classifier learns to predict wrong labels from artifacts with high confidence, making those examples invisible to loss-based detection.[1]

Why Confidence-Based Methods Fail. In artifact-aligned noise, the classifier achieves near-perfect training accuracy by learning the spurious markers. Cleanlab, loss-based, and margin-based methods all rely on mislabeled examples causing low confidence or high loss. But mislabeled examples have *high* confidence (due to markers) and *low* loss, making them rank as the *least* suspicious. This inverts the detection signal, yielding AUROC below 0.5 (worse than random).

ECG vs. ECG (input). Both methods use the same neighborhood surprise algorithm, but on different embeddings:

- **ECG (input)** (0.671): Uses sentence embeddings of the raw input text
- **ECG** (0.832): Uses sentence embeddings of the LLM's explanation (evidence + rationale)

The 24% improvement demonstrates that explanation embeddings capture "why this label" rather than "what this text is about," revealing label inconsistencies invisible in input space.

Multi-Signal Aggregation Hurts. Surprisingly, combining multiple signals (ECG (multi-signal): 0.547) *degrades* performance compared to ECG alone (0.832). We analyze this counterintuitive result in §6.

5.2 Detection Performance on Random Noise

Table 2 shows results on random label noise, where labels are flipped uniformly without artifacts. This is the setting where confidence-based methods are expected to excel.

Two-Regime Comparison. Table 3 summarizes the key finding: **Cleanlab performs well on random noise but poorly on artifact noise**. It achieves near-perfect detection on random noise (0.977 AUROC) but degrades sharply on artifact noise (0.107 AUROC). ECG is robust across both regimes.

5.3 Downstream Improvements

Table 4 shows accuracy after cleaning with ECG. Removing the top 2% of flagged instances yields a +0.57% accuracy improvement.

Precision-Recall Tradeoff. At K=1%, precision is highest (66.8%) but too few noisy examples are

[1] Cleanlab, High-Loss, and AUM show identical AUROC (0.107) because all three methods produce highly correlated rankings based on classifier confidence, and the artifact-induced mislabeled examples are consistently ranked as *least* suspicious across all methods.

K%	Precision	Accuracy	Δ
0% (baseline)	—	93.58%	—
1%	66.8%	93.58%	+0.00%
2%	**57.4%**	**94.15%**	**+0.57%**
5%	40.6%	93.81%	+0.23%
10%	29.7%	93.00%	−0.57%

Table 4: Downstream accuracy after removing top-K% suspicious instances by ECG. Precision indicates what fraction of removed instances were truly mislabeled. K=2% achieves the best accuracy improvement (+0.57%).

Method	5%	10%	20%
Artifact-Aligned Noise			
ECG	0.815	0.832	0.847
ECG (input)	0.658	0.671	0.679
Δ	+0.157	+0.161	+0.168
Random Noise			
ECG	0.931	0.943	0.952
ECG (input)	0.892	0.901	0.908
Δ	+0.039	+0.042	+0.044

Table 5: AUROC across noise rates. ECG's advantage over ECG (input) is consistent and *increases* at higher noise rates for artifact-aligned noise.

removed to impact accuracy. At K=10%, recall is high but precision drops (29.7%), removing too many clean examples. K=2% balances this trade-off.

5.4 Ablation Studies

Noise Rate Sensitivity. Table 5 shows ECG's advantage over ECG (input) is consistent across noise rates (5%, 10%, 20%) and *increases* at higher noise rates on artifact-aligned noise.

Dataset Size Sensitivity. Table 6 shows ECG's advantage is largest on smaller datasets (+0.255 AUROC at 5k vs. +0.161 at 25k).

LLM Size Trade-off. Table 7 shows smaller LLMs (1.7B) produce consistent explanations enabling ECG's best single-method AUROC (0.868), while larger LLMs (14B) enable ensemble methods achieving overall best (0.896).

6 Analysis

Why Explanations Succeed Where Confidence Fails. The fundamental insight behind ECG is that *explanations and classifiers process different information*. When a mislabeled example contains a spurious marker, the classifier learns to predict the wrong label from the marker with high confidence. This is precisely the scenario where confident learning fails (Northcutt et al., 2021a). But the LLM explanation, prompted to ignore metadata tokens, processes the semantic content and cites evidence reflecting the true sentiment. The explanation embedding therefore clusters with semantically similar (correctly labeled) examples, creating high neighborhood surprise.

Method	5k	10k	25k
ECG	0.819	0.827	0.832
ECG (input)	0.564	0.628	0.671
Δ	+0.255	+0.199	+0.161

Table 6: AUROC on artifact-aligned noise across dataset sizes. ECG's advantage is largest on smaller datasets.

Method	1.7B	14B
ECG	**0.868**	0.595
Artifact Detection	0.523	0.687
Ensemble	0.841	**0.896**

Table 7: AUROC by LLM size. Smaller LLMs yield more consistent embeddings benefiting ECG; larger LLMs enable better artifact detection and ensemble performance.

This decoupling is what enables ECG to detect artifact-aligned noise: the classifier exploits shortcuts invisible to the loss surface, but explanations surface the semantic inconsistency. This aligns with findings that explanations can expose artifacts invisible to standard diagnostics (Pezeshkpour et al., 2022; Han et al., 2020).

Why Multi-Signal Aggregation Failed. We initially designed ECG with five complementary signals, expecting that combining them would improve robustness. Instead, multi-signal aggregation (0.547 AUROC) substantially underperformed simple ECG (0.832). The primary culprit is the **training dynamics signal (S_{dyn})**, which is *anti-correlated* with noise under artifact conditions.

The intuition is straightforward: AUM measures how confidently the classifier fits an example. Under artifact-aligned noise, mislabeled examples have spurious markers that make them *easy* to learn: they achieve high confidence and high AUM. Our signal $S_{\text{dyn}} = -\text{AUM}$ therefore assigns *low* suspicion to exactly the examples we want to detect. When combined with other signals, this anti-correlated signal degrades overall performance.

This finding has implications beyond ECG:

training dynamics signals can degrade performance when combined with explanation signals under artifact-driven noise. The failure modes are complementary in theory but antagonistic in practice under this regime.

When to Use ECG vs. Cleanlab. Our results suggest a simple practical guideline:

- If you suspect **random annotation errors** with no systematic pattern, use Cleanlab (AUROC 0.977)

- If you suspect **artifact-aligned noise** or spurious correlations causing confident fitting, use ECG (AUROC 0.832)

- If you are **uncertain about noise type**, ECG is safer: it remains competitive on random noise (0.943) while avoiding catastrophic failure on artifacts

LLM Size Trade-off. Our ablation (Table 7) reveals a fundamental trade-off in LLM-generated explanations for data quality. **Smaller LLMs** (1.7B) produce simpler explanations with less variation across semantically similar examples. This consistency yields more homogeneous explanation embeddings, where ECG can reliably detect label inconsistencies (AUROC 0.868). **Larger LLMs** (14B) produce richer, more nuanced reasoning, but this diversity creates more heterogeneous embeddings that hurt ECG's neighborhood detection (AUROC 0.595). However, larger models excel at explicit artifact detection: the 14B model achieves 0.705 AUROC on artifact detection vs. 0.522 for 1.7B, likely because richer reasoning surfaces spurious patterns more reliably. This enables effective ensemble methods that combine artifact detection with ECG, achieving the best overall AUROC (0.896). The implication is that **explanation model selection should match the detection strategy**: simpler models for ECG's embedding-based detection, larger models for reasoning-based ensemble methods.

Failure Cases and Limitations. ECG struggles with genuinely ambiguous sentences where the LLM is also uncertain. Distinguishing "ambiguous" from "mislabeled" remains challenging, a known difficulty in noisy label detection (Maini et al., 2022). ECG also depends on the LLM correctly ignoring spurious markers. If the LLM itself exploits artifacts, explanations will not reveal inconsistency. We mitigate this through explicit prompting (instructing the LLM to ignore tokens in angle brackets), but future work should explore more robust explanation methods.

Computational Cost. LLM explanation generation is the main bottleneck ($\sim$10 minutes for 25k examples on H100 with vLLM batched inference). Explanations are generated once and cached; subsequent embedding and kNN computation take $<$5 minutes. For larger datasets, selective explanation (only for high-entropy examples) could reduce cost.

7 Conclusion

We introduced Explanation-Consistency Graphs (ECG), demonstrating that neighborhood surprise computed in *explanation embedding space* substantially outperforms the same algorithm on input embeddings for detecting mislabeled training examples. On artifact-aligned noise (where Cleanlab degrades to 0.107 AUROC), ECG achieves 0.832 AUROC, a 24% improvement over ECG (input) (0.671). ECG remains competitive on random noise (0.943 vs. Cleanlab's 0.977), providing a robust method across noise regimes.

Our analysis reveals that the primary value lies in the *explanation representation* rather than complex signal aggregation. Naive multi-signal combination can even degrade performance when training dynamics signals are anti-correlated with artifact-driven noise. This finding offers guidance for future work on combining heterogeneous data quality signals.

By treating explanations as semantic representations for data quality rather than just interpretability outputs, ECG establishes a new paradigm for data-centric NLP.

Limitations

Synthetic Noise. Our primary experiments use synthetic artifact-aligned noise. While this cleanly demonstrates ECG's advantages, real-world annotation artifacts may be more subtle and diverse. Future work should evaluate on naturally-occurring noise patterns.

Single Dataset. We evaluated exclusively on SST-2 sentiment classification. While SST-2 is a standard benchmark, generalization to other domains (e.g., NLI, question answering, named entity recognition) and languages remains to be demonstrated.

LLM Dependence. ECG relies on the LLM generating faithful, structured explanations. If the LLM systematically fails on certain instance types (e.g., sarcasm, negation), those failures propagate. We mitigate this with stability sampling, but more robust explanation verification remains important.

Single-Run Results. We report results from single experimental runs without error bars or confidence intervals. While our main findings show large effect sizes (e.g., 0.832 vs 0.107 AUROC), future work should include multiple runs with different random seeds to quantify variance.

Computational Cost. Generating explanations for large datasets (millions of examples) may be prohibitive. Strategies like selective explanation (only for high-entropy examples) could reduce cost.

Binary Classification. We evaluated on binary sentiment classification. Extension to multi-class and structured prediction tasks requires adapting the graph construction and scoring mechanisms.

Ethical Considerations

Training data debugging can improve model fairness by identifying and correcting label biases. However, automated cleaning may inadvertently remove minority viewpoints or reinforce majority biases if the LLM itself exhibits biases. We recommend human review of flagged instances, especially for sensitive domains.

Use of AI Assistants. AI writing assistants were used for code debugging, LaTeX formatting, and editorial suggestions during manuscript preparation. All scientific contributions, experimental design, methodology, and analysis are the authors' original work.

References

Chirag Agarwal et al. 2024. Faithfulness vs. plausibility: On the (un)reliability of explanations from large language models. *arXiv preprint arXiv:2402.04614*.

Dara Bahri, Heinrich Jiang, and Maya Gupta. 2020. Deep k-nn for noisy labels. In *International Conference on Machine Learning*, pages 540–550.

Yonatan Belinkov, Adam Poliak, Stuart Shieber, Benjamin Van Durme, and Alexander Rush. 2019. Don't take the premise for granted: Mitigating artifacts in natural language inference. In *Proceedings of ACL*.

Luca Beurer-Kellner, Marc Fischer, and Martin Vechev. 2024. Guiding llms the right way: Fast, non-invasive constrained generation. *arXiv preprint arXiv:2403.06988*.

Yanda Chen, Ruiqi Chan, Zexuan Wang, Kathleen McKeown, and Wei Xu. 2025. Explanation consistency finetuning. *arXiv preprint arXiv:2401.13986*.

Derek Chong, Jenny Hong, and Christopher D. Manning. 2022. Detecting label errors by using pre-trained language models. In *Proceedings of EMNLP*.

Ching-Yao Chuang, R Devon Hjelm, Xin Wang, Vibhav Vineet, Neel Joshi, Antonio Torralba, Stefanie Jegelka, and Yale Song. 2022. Robust contrastive learning against noisy views. In *CVPR*.

Christopher Clark, Mark Yatskar, and Luke Zettlemoyer. 2019. Don't take the easy way out: Ensemble based methods for avoiding known dataset biases. In *Proceedings of EMNLP-IJCNLP*, pages 4069–4082.

Francesco Di Salvo, Diego Doimo, Alessandro Sierra, Alberto Cazzaniga, Luca Moschella, Emanuele Rodolà, Francesco Locatello, and Priya Goyal. 2025. An embedding is worth a thousand noisy labels. *Transactions on Machine Learning Research*.

Saibo Geng, Martin Josifoski, Maxime Peyrard, and Robert West. 2023. Grammar-constrained decoding for structured nlp tasks without finetuning. *arXiv preprint arXiv:2305.13971*.

Suchin Gururangan, Swabha Swayamdipta, Omer Levy, Roy Schwartz, Samuel Bowman, and Noah A Smith. 2018. Annotation artifacts in natural language inference data. In *Proceedings of NAACL-HLT*, pages 107–112.

Xiaochuang Han, Byron C Wallace, and Yulia Tsvetkov. 2020. Explaining black box predictions and unveiling data artifacts through influence functions. In *Proceedings of ACL*.

Shiyuan Huang, Siddarth Mamidanna, Shreedhar Jangam, Yilun Zhou, and Leilani H. Gilpin. 2023. Can large language models explain themselves? a study of llm-generated self-explanations. *arXiv preprint arXiv:2310.11207*.

Ahmet Iscen et al. 2020. Graph convolutional networks for learning with few clean and many noisy labels. In *European Conference on Computer Vision*.

Divyansh Kaushik, Eduard Hovy, and Zachary C Lipton. 2020. Learning the difference that makes a difference with counterfactually-augmented data. In *International Conference on Learning Representations*.

Jang-Hyun Kim, Sangdoo Yun, and Hyun Oh Song. 2023. Neural relation graph: A unified framework for identifying label noise and outlier data. *arXiv preprint arXiv:2301.12321*.

Woosuk Kwon, Zhuohan Li, Siyuan Zhuang, Ying Sheng, Lianmin Zheng, Cody Hao Yu, Joseph Gonzalez, Hao Zhang, and Ion Stoica. 2023. Efficient memory management for large language model serving with PagedAttention. In *Proceedings of the 29th Symposium on Operating Systems Principles*, pages 611–626.

Dong-Ho Lee, Seonghyeon Shin, Seung-won Kim, and Minjoon Seo. 2023. Xmd: An end-to-end framework for interactive explanation-based debugging of nlp models. In *Proceedings of ACL*.

Piyawat Lertvittayakumjorn, Lucia Specia, and Francesca Toni. 2020. Find: Human-in-the-loop debugging deep text classifiers. In *Proceedings of EMNLP*, pages 332–348.

Piyawat Lertvittayakumjorn and Francesca Toni. 2021. Explanation-based human debugging of nlp models: A survey. *Transactions of the Association for Computational Linguistics*, 9:1508–1528.

Dongxu Li, Wei Zhang, and Yang Liu. 2025. Decole: Decoupled confident learning for mislabeling detection. *arXiv preprint arXiv:2507.07216*.

Andreas Madsen, Siva Reddy, and Sarath Chandar. 2024. Are self-explanations from large language models faithful? *arXiv preprint arXiv:2401.07927*.

Pratyush Maini, Saurabh Garg, Zachary Lipton, and J Zico Kolter. 2022. Characterizing datapoints via second-split forgetting. In *Advances in Neural Information Processing Systems*.

R Thomas McCoy, Ellie Pavlick, and Tal Linzen. 2019. Right for the wrong reasons: Diagnosing syntactic heuristics in natural language inference. In *Proceedings of ACL*.

Curtis Northcutt, Lu Jiang, and Isaac Chuang. 2021a. Confident learning: Estimating uncertainty in dataset labels. *Journal of Artificial Intelligence Research*, 70:1373–1411.

Curtis G Northcutt, Anish Athalye, and Jonas Mueller. 2021b. Pervasive label errors in test sets destabilize machine learning benchmarks. *arXiv preprint arXiv:2103.14749*.

Letitia Parcalabescu et al. 2024. Measuring faithfulness in chain-of-thought reasoning. In *Proceedings of ACL*.

Pouya Pezeshkpour, Sarthak Jain, Byron C Wallace, and Sameer Singh. 2022. Combining feature and instance attribution to detect artifacts. In *Findings of ACL*.

Geoff Pleiss, Tianyi Zhang, Ethan Elenberg, and Kilian Q Weinberger. 2020. Identifying mislabeled data using the area under the margin ranking. In *Advances in Neural Information Processing Systems*, volume 33, pages 17044–17056.

Adam Poliak, Jason Naradowsky, Aparajita Halber, Rachel Rudinger, and Benjamin Van Durme. 2018. Hypothesis only baselines in natural language inference. In *Proceedings of *SEM*, pages 180–191.

Korbinian Randl et al. 2024. Self-explanation evaluation of llms. *arXiv preprint arXiv:2407.14487*.

Shiori Sagawa, Pang Wei Koh, Tatsunori B Hashimoto, and Percy Liang. 2020. Distributionally robust neural networks for group shifts: On the importance of regularization for worst-case generalization. In *International Conference on Learning Representations*.

Qwen Team. 2025. Qwen3 technical report. *arXiv preprint arXiv:2505.09388*.

Stefano Teso et al. 2021. Interactive label cleaning with example-based explanations. In *Advances in Neural Information Processing Systems*.

Aravind Thyagarajan, Einar Snorrason, Curtis Northcutt, and Jonas Mueller. 2022. Identifying incorrect annotations in multi-label classification data. *arXiv preprint arXiv:2211.13895*.

Lifu Tu, Garima Lalwani, Spandana Gella, and He He. 2020. An empirical study on robustness to spurious correlations using pre-trained language models. In *Transactions of the Association for Computational Linguistics*.

Prasetya Ajie Utama, Nafise Sadat Moosavi, and Iryna Gurevych. 2020. Mind the trade-off: Debiasing nlu models without degrading the in-distribution performance. In *Proceedings of ACL*.

Wei-Chen Wang and Jonas Mueller. 2022. Detecting label errors in token classification data. *arXiv preprint arXiv:2210.03920*.

Sarah Wiegreffe, Ana Marasović, and Noah A Smith. 2021. Measuring association between labels and free-text rationales. In *Proceedings of EMNLP*.

Congying Xia, Chen Xing, Jiangshu Du, Xinyi Yang, Yihao Feng, Ran Xu, Wenpeng Yin, and Caiming Xiong. 2024. Fofo: A benchmark to evaluate llms' format-following capability. *arXiv preprint arXiv:2402.18667*.

Tianyang Xu et al. 2024. Sayself: Teaching llms to express confidence with self-reflective rationales. *arXiv preprint arXiv:2405.20974*.

Bo Yuan, Jie Chen, Yitong Wang, and Shibo Wang. 2025. Label distribution learning-enhanced dual-knn for text classification. *arXiv preprint arXiv:2503.04869*.

Chang Yue and Niraj K. Jha. 2022. Ctrl: Clustering training losses for label error detection. *arXiv preprint arXiv:2208.08464*.

Zhaowei Zhu, Yao Song, Jiangchao Liu, Jingfeng Zhao, and Yang Liu. 2022. Detecting corrupted labels without training a model to predict. In *International Conference on Machine Learning*.

A Explored Multi-Signal Extensions

In addition to neighborhood surprise (S_{nbr}), we explored four additional signals. While theoretically motivated, combining them with S_{nbr} degraded performance on artifact-aligned noise. We document them here for completeness.

NLI Contradiction (S_{nli}). If an explanation *contradicts* the observed label according to an NLI model, the label may be wrong. We form premise t_i (explanation text) and hypothesis $h(y_i)$ ("The sentiment is [label]."), then compute:

$$S_{\text{nli}}(i) = P_{\text{contradict}} - P_{\text{entail}} \tag{6}$$

using an ensemble of NLI models (RoBERTa-large-MNLI, BART-large-MNLI).

Artifact Focus (S_{art}). If the LLM's cited evidence contains known spurious tokens:

$$S_{\text{art}}(i) = \frac{|\text{Tokens}(\text{evidence}_i) \cap \mathcal{S}|}{|\text{Tokens}(\text{evidence}_i)|} \tag{7}$$

where $\mathcal{S}$ is the set of known spurious tokens.

Instability (S_{stab}). High explanation variance may indicate ambiguous instances:

$$S_{\text{stab}}(i) = 1 - \rho_i \tag{8}$$

where ρ_i is the reliability score from stability sampling.

Training Dynamics (S_{dyn}). Low AUM indicates the classifier struggles with this example:

$$S_{\text{dyn}}(i) = -\text{AUM}(i) \tag{9}$$

Why Aggregation Failed. Under artifact-aligned noise, S_{dyn} is *anti-correlated* with noise because artifacts make mislabeled examples easy to learn (high AUM). When combined via weighted averaging, this anti-correlated signal degrades overall detection. Future work should explore noise-regime-aware signal selection.

B Implementation Details

Hyperparameters. Table 8 lists all hyperparameters used in experiments.

Parameter	**Value**
Classifier	
Model	RoBERTa-base
Learning rate	2e-5
Batch size	64
Epochs	3
Max length	128
Explanation	
LLM	Qwen3-8B
Primary temperature	0.0
Sample temperature	0.7
Stability samples	3
Max new tokens	150
Graph	
Embedding model	all-MiniLM-L6-v2
k (neighbors)	15
Temperature τ	0.07
Similarity threshold	0.35
Signals	
NLI models	RoBERTa-large-MNLI, BART-large-MNLI
Smoothing ϵ	1e-3

Table 8: Hyperparameters for all experiments.

Prompt Template. The LLM prompt for explanation generation is:

```
You are a careful annotator.

Task: classify the sentiment of the
INPUT as POSITIVE or NEGATIVE.

IMPORTANT: Ignore any metadata tokens
in angle brackets like <lbl_pos>,
<lbl_neg>.

Return ONLY valid JSON with keys: -
"pred_label": "POSITIVE" or "NEGATIVE"
- "evidence": array of 1-3 EXACT
substrings - "rationale": one sentence,
≤25 tokens - "counterfactual": minimal
change to flip sentiment - "confidence":
integer 0-100

INPUT: {sentence}
```

C Supplementary Related Work

This appendix provides extended discussion of related work topics that support but are not central to ECG's main positioning.

C.1 Extensions of Confident Learning

Confident learning has been adapted beyond standard classification to diverse settings. Token-level label error detection extends the confident joint formulation to NER, where individual tokens rather than full sequences may be mislabeled (Wang and Mueller, 2022). Multi-label classification requires handling the combinatorial label space and partial label noise (Thyagarajan et al., 2022). Label-biased settings, where annotator bias patterns systematically correlate with certain features, require decoupling bias patterns from noise detection (Li et al., 2025). These extensions demonstrate the broad applicability of confidence-based detection but inherit the same fundamental limitation: reliance on mislabeled examples causing low confidence.

C.2 Additional Training Dynamics Signals

Beyond AUM and CTRL-style dynamics, second-split forgetting (Maini et al., 2022) characterizes datapoints by how quickly they are forgotten during continued training on a held-out split. Examples that are rapidly forgotten after initial learning may be mislabeled or atypical. This provides an alternative view of "hard-to-learn" examples that complements margin-based approaches, though it still relies on training signals that become unreliable under artifact-aligned noise.

C.3 Robust Graph Construction in NLP

Graph-based cleaning depends critically on embedding quality, and NLP embeddings may be noisier or less well-calibrated than vision-style features (Zhu et al., 2022). Several approaches address this challenge. Dual-kNN methods combine text embeddings with label-probability representations to create more stable neighbor definitions under noise (Yuan et al., 2025). Robust contrastive learning addresses noise in positive pairs by explicitly modeling and downweighting likely-corrupted pairs during representation learning (Chuang et al., 2022). These techniques could potentially be combined with ECG's explanation embeddings to further improve robustness.

C.4 LLM-Generated Explanations: Structure and Reliability

Structured Output Generation. Generating structured explanations from LLMs requires format reliability. **Grammar-constrained decoding** guarantees outputs match a target schema (Geng et al., 2023), essential when downstream processing is brittle to parsing failures. Subword-aligned constraints reduce accuracy loss from token-schema misalignment (Beurer-Kellner et al., 2024). The FOFO benchmark reveals that strict format-following is a non-trivial failure mode for open models (Xia et al., 2024), motivating our use of schema-guaranteed generation rather than prompt-only formatting.

Faithfulness and Plausibility. A central concern with LLM explanations is that plausible explanations may not be faithful to the model's actual reasoning (Agarwal et al., 2024). Faithfulness varies by explanation type and model family (Madsen et al., 2024). Self-consistency checks can test whether different explanation types are faithful to the decision process (Randl et al., 2024). Perturbation tests offer a direct route to faithfulness: if an explanation claims feature X is important, removing X should change the prediction (Parcalabescu et al., 2024). ECG addresses faithfulness concerns not by assuming explanations are faithful, but by *verifying* them through neighborhood agreement: if an explanation's embedding clusters with correctly-labeled examples, the explanation is likely meaningful regardless of whether it captures the LLM's "true" reasoning.

Explanation Stability and Uncertainty. LLM explanations can be unstable across prompts and random seeds. Explanation-consistency finetuning improves stability across semantically equivalent inputs (Chen et al., 2025). **SaySelf** trains models to produce calibrated confidence and self-reflective rationales using inconsistency across sampled reasoning chains (Xu et al., 2024). These findings motivate ECG's stability sampling and reliability weighting: by generating multiple explanations per instance and measuring agreement, we can identify instances where the LLM is uncertain and downweight their contribution to neighborhood signals.

Label Leakage in Rationales. Rationales can correlate with labels in ways enabling leakage, where a model can predict the label from the rationale without looking at the input (Wiegreffe et al., 2021). ECG addresses this by forbidding label words in rationales (enforced via the JSON schema) and constructing embeddings from evidence and rationale text that excludes the predicted label.